Laboratori Nazionali di Frascati

LNF-92/025 (P)
9 Aprile 1992

ENSLAPP-A-375/92

J.L. Franzini, W. Kim, P.J. Franzini

RADIATIVE ϕ DECAYS: EXPERIMENTAL PROBLEMS

Contribution to the DAΦNE Physics Handbook

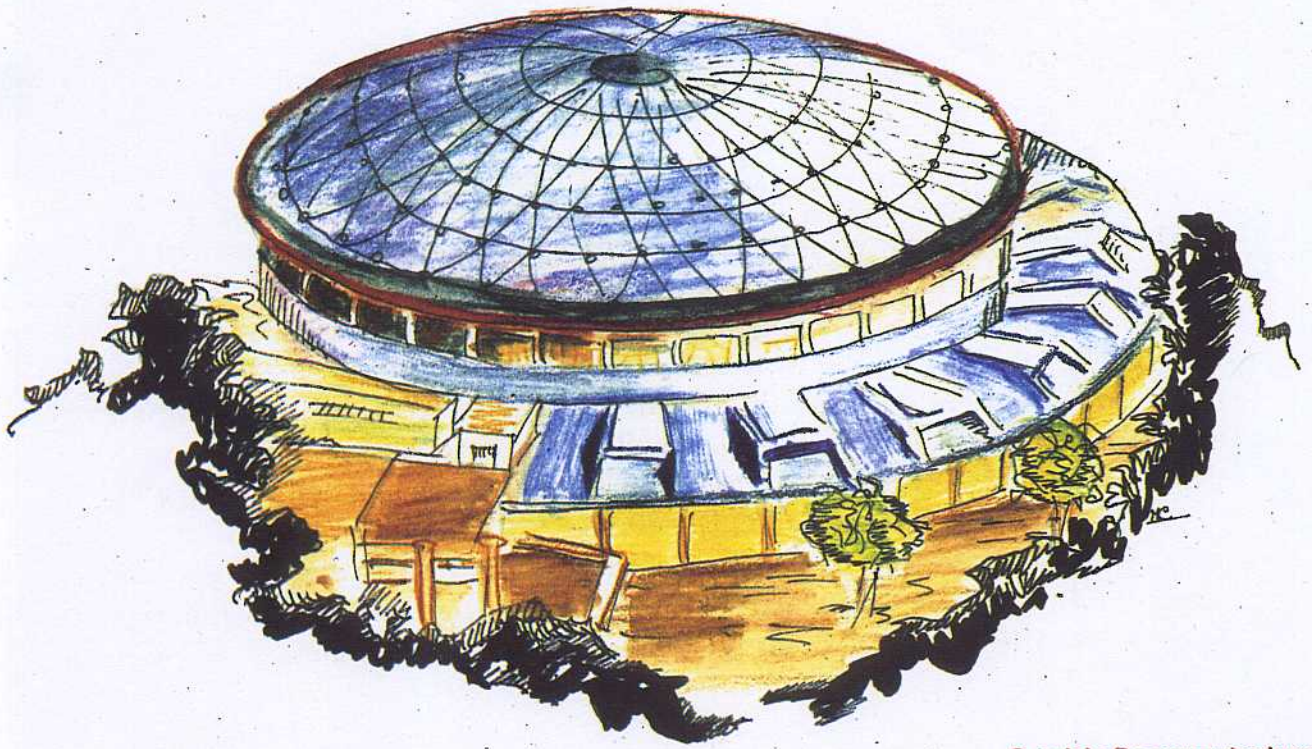

Servizio Documentazione
dei Laboratori Nazionali di Frascati
P.O. Box, 13 - 00044 Frascati (Italy)

INFN - Laboratori Nazionali di Frascati
Servizio Documentazione

LNF-92/025 (P)
9 Aprile 1992

ENSLAPP-A-375/92

RADIATIVE ϕ DECAYS: EXPERIMENTAL PROBLEMS

JULIET LEE-FRANZINI

Laboratori Nazionali di Frascati dell'INFN

SUNY at Stony Brook, Stony Brook, New York 11794

WON KIM

SUNY at Stony Brook, Stony Brook, New York 11794

PAULA J. FRANZINI

Laboratoire D'Annecy-Le-Vieux de Physique des Particules, Annecy, France

ABSTRACT

Experimental issues associated with measuring rare ϕ radiative decays at DAΦNE are discussed. We have studied by Monte Carlo simulation the detection of $\phi \to f_0\gamma$, both for $f_0 \to \pi^0\pi^0$and $f_0 \to \pi^+\pi^-$, in a minimal high precision spectrometer, CUSB. We find that, BR's as small as 1×10^{-6} are measurable if all final particles are neutral, even assuming BR($\phi \to \pi^0\pi^0\gamma$) is 10^{-3}, the experimental upper limit. We find, that the general purpose detector KLOE will achieve even higher accuracy, because of its hermeticity and fine segmentation. For $f_0 \to \pi^+\pi^-$, we found that CUSB's sensitivity is limited to BR's of the order of 10^{-5}, whereas KLOE is sensitive to the smallest expected BR. We have included in the analysis the background process $e^+e^- \to \phi \to \pi\pi\gamma$, via a $\rho\pi$ intermediate state. The matrix element and angular distributions for this process are given in the appendix. We also find that KLOE can measure the BR($\phi \to \eta'\gamma$) down to $\sim10^{-6}$.

1. INTRODUCTION

DAΦNE,[1] beginning in 1995, will deliver a luminosity $\mathcal{L}\sim10^{32}$ cm^{-2} s^{-1}. At such values of $\mathcal{L}$, of the order of 5 billion ϕ's are produced in four months of machine-on time: $5[\mu b]\times10^{32}[cm^{-2}\ s^{-1}]\times10^{7}$ [s]$=5\times10^{9}$. In the following we assume that 5×10^{9} ϕ mesons are collected in the first year, while DAΦNE is tuned to reach maximum $\mathcal{L}$. This constitutes an enormously large sample of ϕ's, previously unavailable, and gives the possibility of detecting rare ϕ decays, especially rare radiative decays which typically are predicted to have branching ratio's (BR) of the order of 10^{-4} to 10^{-7}.[2] Existing experimental measurements are few. The most common radiative mode is $\phi\rightarrow\eta^0\gamma$ with BR($\phi\rightarrow\eta^0\gamma$)$=0.0128\pm0.0006$; the next most frequent mode $\phi\rightarrow\pi^0\gamma$ is measured to an accuracy of only 30%: BR($\phi\rightarrow\pi^0\gamma$)$=(0.31\pm0.13)\times10^{-3}$.[3] Many modes which are not forbidden by symmetry arguments, but are very interesting from a spectroscopic point of view, such as $\phi\rightarrow\eta'\gamma$, $\rightarrow f_0\gamma$, $\rightarrow a_0\gamma$, $\rightarrow\pi^+\pi^-\gamma$, $\rightarrow\pi^0\pi^0\gamma$, $\rightarrow\pi^0\eta\gamma$, have not been observed at all and upper limits of the order of 10^{-3} are given. About the C violating decays $\phi\rightarrow\omega\gamma$, $\rightarrow\rho\gamma$, $\rightarrow\eta\pi^0$ we know nothing; upper limits are of the order of 10^{-2}.[3] We discuss in the following detector issues associated with measuring rare radiative decays amidst prolific background events arising from $\phi\rightarrow X+\pi^0(\rightarrow 2\gamma)$ decays, with specific examples of $\phi\rightarrow f_0\gamma$ and $\phi\rightarrow\eta'\gamma$.

2. SPECTROSCOPY DETECTORS

2.1 Precision EM Calorimeters

Spectroscopy requiring detection of neutral particles in the final state has been done in the more recent past with dedicated electromagnetic calorimeters, often composed of scintillating crystals (NaI, BGO, CsI) which give excellent photon energy resolution. Typically a minimal level of tracking with no magnetic field is provided, thus there is no momentum determination for charged particles. This allows to distinguish between charged and neutral particles, and gives the direction of charged particles and the entry point of tracks into the calorimeter. To reconstruct the neutral particles (π^0, η etc.), whose decay products include photons, it is necessary to determine the direction of the final state photons. This is obtained by segmenting the calorimeter into many polar and azimuthal elements to find the electromagnetic (EM) shower centroid to the required accuracy. With highly segmented calorimeters, particle identification is accomplished by recognizing the characteristic energy deposition patterns of particles in the crystals. EM showers from an electron or photon have typical longitudinal and transverse profiles which allow rejection of spurious signals to the 10^{-2} - 10^{-3} level. Minimum

ionizing particles have constant energy deposition along their paths. Strongly interacting particles, hadrons, may undergo nuclear interactions in the crystals, exhibiting a discontinuous energy deposition pattern at the point of interaction. If the calorimeter is longitudinally segmented finely enough, particle identification can also be aided by range measurements. The most crucial considerations in obtaining the ideal energy resolution from these calorimeters is to have

1. constant monitoring of the crystal to crystal calibrations, and
2. a precise overall energy scale determination.

The implementation of a neutral particle spectrometer at one of DAΦNE's interaction regions is highly desirable because

1. the luminosity required for spectroscopy studies is less than that required for CP violation studies,
2. neutral particle calorimeters are compact and easier to install and become operational, especially if one transports to DAΦNE a proven world-class spectrometer which can be recycled at the time of DAΦNE's commissioning.

We chose the CUSB-II Spectrometer[4] for our Monte Carlo (MC) feasibility studies of measuring rare radiative ϕ decays at DAΦNE with a neutral particle spectrometer. After the completion of upsilon spectroscopy studies at CESR for a decade, CUSB has been disassembled, packed in crates, stored *in toto* at the Nevis Laboratories and is available for being reconstituted at DAΦNE if needed.

2.2 General Purpose Detectors

These detectors consist of large tracking devices in magnetic field and EM calorimeters inside or outside the coil producing the field. They can measure energy or momenta of charged and neutral particles as well, usually with lower precision for photons, but compensate for this by more complete sensitivity to the full event topology and kinematics. We will quote in a following section the results of a MC study of the sensitivity to a rare radiative ϕ decay of an operating magnetic spectrometer, the CMD2.[5] We also remark on the sensitivity of a new general purpose detector which has the EM calorimeter inside the coil, KLOE,[6] which is being designed for operations at DAΦNE.

3. $\phi \rightarrow f_0\gamma$

3.1 $f_0 \rightarrow \pi^0\pi^0$

We chose for our MC studies the reaction $\phi \rightarrow f_0\gamma$, where the f_0 decays into a $\pi^+\pi^-$ pair or into two π^0's. The branching ratio for this reaction is interesting because of:

1. the implications it has for the measurement of $\Re(\epsilon'/\epsilon)$ and$\Im(\epsilon'/\epsilon)$,
2. the value it has in its own right from a spectroscopic point of view. See the discussion of Brown and Close[2] in this report.

This decay has not been observed yet. The experimental limit is of the order of 2×10^{-3}, which is much higher than the most optimistic theoretical expectation of 2.5×10^{-4}.[7] Partial wave analysis suggests that 78% of the f_0's decay to two pions (1/3 neutral, 2/3 charged), 22% to a pair of K's.

The signature for the decay $\phi \rightarrow f_0\gamma$, $f_0 \rightarrow \pi^0\pi^0$ is five photons, with one of the photons having ~50 MeV and four of the photons reconstructing to a pair of nearly collinear π^0's, whose invariant mass sums up to that of the f_0. The possible background events are from:

1. $\phi \rightarrow \pi^0\pi^0\gamma$, experimentally not yet detected, with an upper limit of BR$<1\times10^{-3}$. Measured values in this paper are taken from the Particle Data Book[3] unless otherwise specified. Predicted values for this process via a virtual ρ vary from 1.2×10^{-5},[8,9] to 3.62×10^{-5}.[10]
2. $\phi \rightarrow \pi^0\rho^0$ with $\rho \rightarrow \pi^0\gamma$. The product branching ratio of these two observed processes is BR$=(3.4\pm0.88)\times10^{-5}$.
3. $\phi \rightarrow \pi^0\rho^0$ with $\rho \rightarrow \eta\gamma$, $\eta \rightarrow 2\gamma$, with the product BR from the three observed processes, BR$=(6.4\pm1.2)\times10^{-6}$, all of which yield five photons.
4. $\phi \rightarrow \gamma\eta$ with $\eta \rightarrow 3\pi^0$, with product BR from the observed two processes: BR $=(4.1\pm2.0)\times10^{-3}$, and two of the photons not detected in the calorimeter.

There is no background arising from $\phi \rightarrow K_S K_L$ where the K_S decays into 2 π^0's and the K_L decays into 3 π^0's and five photons are missed. The (acceptance$\times K_L$ decay probability)$\times$BR, A, in CUSB is 5.8×10^{-5}, in KLOE 3.1×10^{-10}. This is before applying any energy-momentum constraint.

To be on the conservative side, we have considered background (1) both at the estimated level found theoretically in Refs. 8 and 9, and at the much larger level allowed by the current experimental bound. We have treated background (2) separately from

background (1) because it can be best dealt with experimentally using the constraint of a physical ρ. Moreover, we suspect that the theoretical estimate of background (1) in Refs. 8 and 9 might be low by a factor of two or three since the estimates in the same model for the $\phi \to \pi^0\rho^0$ and $\rho \to \pi^0\gamma$ branching ratios are also low. $\phi \to \pi\rho \to \pi\eta\gamma$ can also be treated similarly as background (1). If we use the theoretical estimate via a virtual ρ,[9] (3) is negligible; if we use the experimental value, it is a similar exercise to that of considering background (1).

Using the CUSB Monte Carlo program, signal and background processes were generated and the particles followed through in the CUSB spectrometer. For the $\phi \to \pi^0\pi^0\gamma$ process we have used the matrix elements with angular distributions from reference 8. For completeness of the DAΦNE Physics Handbook, we include them in this paper in the appendix. Photon spectra and acceptance$\times$detection efficiencies (ϵ) for each process were obtained after applying the following selection criteria: five and only five photons are present in the detector; four of the photons are paired into two π^0's whose reconstructed mass must be within 50 MeV of the π^0 mass; the reconstructed f_0 mass from the two pions must be within 50 MeV of the expected mass peak at 975 MeV; the energy of the leftover photon is to be less than 95 MeV, and, finally, the invariant mass of all the decay products must be within 50 MeV of the known ϕ mass. ϵ for the signal in CUSB is $(9.7\pm0.1)\times10^{-2}$. This small CUSB value arises from the fact that CUSB central calorimeter covers a solid angle of $0.7\times4\pi$, which results in a geometrical acceptance for five photons of 0.17 (to be contrasted with KLOE which covers over 98% of 4π, thus resulting in a geometrical acceptance for five photons of 0.92). The application of kinematical cuts, reconstruction of pions, and f_0, etc., account for the rest of the loss. CUSB has superb photon energy resolution, which is given by $\sigma(E_\gamma)/E_\gamma = 2\%/\sqrt[4]{E_\gamma}$ where E_γ is measured in GeV. The compensation for applying all the selection criteria in CUSB is that the ϵ for backgrounds 1–3 are down by about a factor of 42, and, background (4) is negligible. Table Ia summarizes the experimental numbers.

Table Ia. BR and ϵ for neutral signal and backgrounds in CUSB and KLOE

PROCESS	BR	ϵ_{CUSB}	ϵ_{KLOE}
$\phi\rightarrow f_0\gamma\rightarrow\pi^0\pi^0\gamma$	$(0.26\rightarrow 65)\times 10^{-6}$	9.7×10^{-2}	8.4×10^{-1}
$\phi\rightarrow\pi^0\pi^0\gamma$	$(1.2\rightarrow 100)\times 10^{-5}$	1.5×10^{-4}	1.3×10^{-3}
$\phi\rightarrow\pi^0\rho^0\rightarrow\pi^0\pi^0\gamma$	3.4×10^{-5}	4.4×10^{-3}	8.4×10^{-4}
$\phi\rightarrow\pi^0\rho^0\rightarrow\pi^0\eta\gamma$	6.4×10^{-6}	1.0×10^{-3}	8.4×10^{-4}
$\phi\rightarrow\gamma\eta\rightarrow 3\pi^0\gamma$	4.1×10^{-3}	1.5×10^{-7}	$<1\times 10^{-7}$

All spectra of background photon surviving the cuts were fitted to polynomials, $g(k)$ where k is the photon energy. The signal has a Breit-Wigner form, $s(k)$. Using the *a priori* error estimate,[11] the fractional accuracy of the signal BR is given by:

$$\frac{\delta(\mathrm{BR})}{\mathrm{BR}} = \frac{1}{\mathrm{BR}}\frac{1}{\sqrt{N}}\Big(\int\frac{1}{f(k)}\Big(\frac{\partial f(k;\mathrm{BR})}{\partial \mathrm{BR}}\Big)^2 \mathrm{d}k\Big)^{-\frac{1}{2}} \tag{3.1}$$

where

$$f(k) = \sum_1^4 \epsilon_{bcknd,i}\times \mathrm{BR}_{bcknd,i}\times g_i(k) + \epsilon_{signal}\times \mathrm{BR}_{signal}\times s(k).$$

Thus, in a year's run at DAΦNE ($\sim 5\times 10^9$ ϕ's), CUSB can measure the BR($\phi\rightarrow f_0\gamma$), using the two $\pi^0\pi^0$ decay mode, from 2% to 36% accuracy over the expected range of theoretical predictions if the BR of direct $\phi\rightarrow\pi^0\pi^0\gamma$ is the one expected theoretically. If the direct $\phi\rightarrow\pi^0\pi^0\gamma$ BR is at the experimental limit the smallest signal BR that CUSB can measure to 5 sigma accuracy is 1.0×10^{-6}, which means that any good spectrometer can access the smallest branching ratio. These results are tabulated in Table Ib.

Applying the same selection criteria in KLOE, the loss in signal is much less severe, because for this particular decay involving five photons from a wide parent signal (f_0) peak, it is more important for kinematical fitting and reconstruction to have small photon losses than extremely precise energy resolution. KLOE's photon resolution is given by $\sigma(E_\gamma)/E_\gamma = 6\%/\sqrt{E_\gamma}$ where E_γ is measured in GeV. KLOE's ϵ for the f_0's neutral decay mode we estimate to be 84%, 30 times better than CUSB.[12] The accuracy attainable by KLOE in the same corresponding period is shown in the last column of table Ib. One expects superb sensitivities to the signal over the whole range of signal and background BR's examined.

Table Ib. Fractional error in BR($\phi \rightarrow f_0\gamma$) for CUSB and KLOE

BR($\phi \rightarrow f_0\gamma$)	BR($\phi \rightarrow \pi^0\pi^0\gamma$)	δ(BR)/BR CUSB	δ(BR)/BR KLOE
1.0×10^{-6}	1.2×10^{-5}	0.140	0.025
2.5×10^{-4}	1.2×10^{-5}	0.004	0.002
1.0×10^{-6}	1.0×10^{-3}	0.180	0.044
2.5×10^{-4}	1.0×10^{-3}	0.005	0.0015

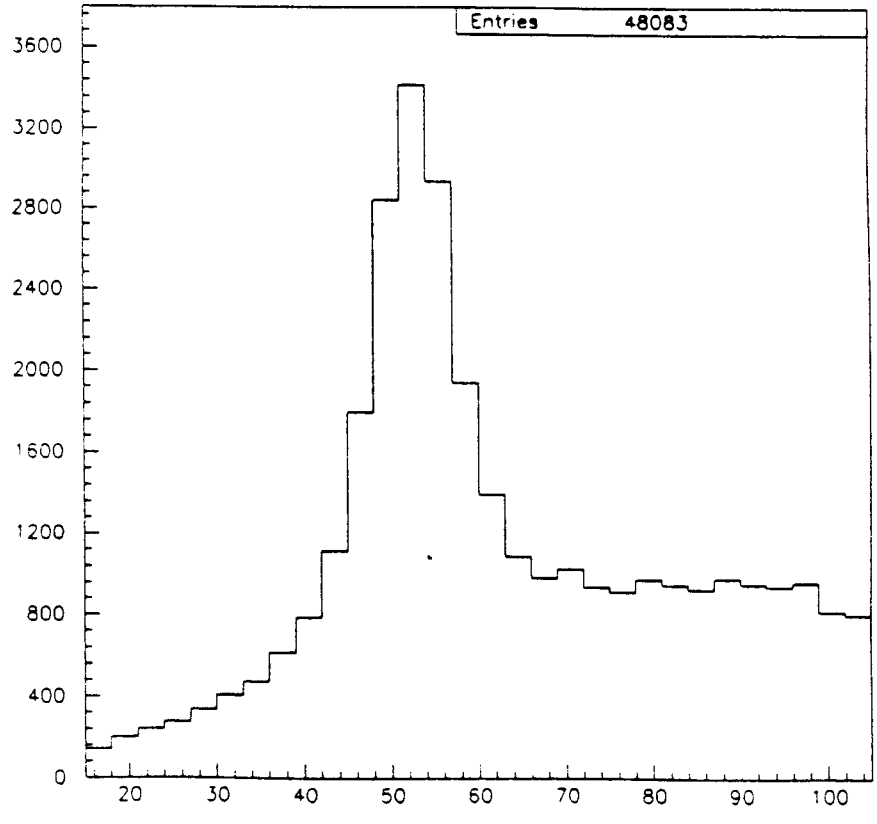

Figure 1. Photon Spectrum in CUSB from $\phi \rightarrow f_0\gamma$.

Figure 1 shows the photon spectrum in CUSB from one year's run with BR($\phi \rightarrow f_0\gamma$) = 2.5×10^{-4} and BR($\phi \rightarrow \pi^0\pi^0\gamma$)= 1×10^{-3}.

3.2 $f_0 \rightarrow \pi^+\pi^-$

The signature for $\phi \rightarrow f_0\gamma$, $f_0 \rightarrow \pi^+\pi^-$ is a pair of nearly collinear charged pions, whose invariant mass equals that of the f_0, and one low energy photon. The possible backgrounds from ϕ decay are

1. $\phi \to \pi^+\pi^-\gamma$, for which the experimental limit is BR$<7\times10^{-3}$. The computed BR value, via a virtual ρ, is twice that for the neutral mode given in the previous section,[13] or from 2.4×10^{-5},[8] to 7.24×10^{-5}.[14]
2. $\phi \to \pi^+\pi^-\pi^0$, BR$=(1.9\pm1.1)\times10^{-2}$.
3. $\phi \to \pi^0\rho^0 \to \pi^0\pi^+\pi^-$, product BR$= (4.3\pm0.2)\times10^{-2}$.
4. $\phi \to \pi^\pm\rho^\mp \to \pi^0\pi^+\pi^-$, product BR$=(8.6\pm0.5)\times10^{-2}$.

The last three reactions yield two oppositely charged pions and one neutral pion, so contribute to the background if one photon is not detected.

There is no background arising from $\phi \to K_S K_L$ where the $K_S \to \pi^+\pi^-$and $K_L \to 3\pi^0$'s and five photons are not detected. A for CUSB is of the order of 1.2×10^{-5}, and for KLOE it is 1.7×10^{-11}. Nor is there from $\phi \to K_S K_L$ where $K_S \to \pi^0\pi^0$ and $K_L \to \pi^+\pi^-\pi^0$ or $\pi^\pm\mu^\mp\nu$, and five or three photons are undetected. A for CUSB is of the order of 3.3×10^{-6} and 5.3×10^{-5} for the two processes; for KLOE the corresponding A's are 4.5×10^{-12} and 5.4×10^{-8}. Finally, there is also no background arising from $\phi \to K_S K_L$ where the $K_S \to \pi^+\pi^-$and $K_L \to \gamma\gamma$ and one photon is not detected. A for CUSB is of the order of 1.4×10^{-6}, for KLOE 1×10^{-6}. All these numbers are obtained before applying the energy-momentum conservation constraint.

Again, signal and background processes were simulated in the CUSB spectrometer. For $\phi \to \pi^+\pi^-\gamma$ we have used the matrix elements with angular distributions from reference 8, which are also in the appendix. We used the following selection criteria: two tracks and one photon are present in the detector; the opening angle between the two tracks is within 2° of 175°; the energy of the photon is within 10 MeV of 53 MeV. Using again the *a priori* error estimate[11] with the fitted background polynomials and the above quoted BR's, in a year's run at DAΦNE ($\sim 1.5 \times 10^9 \phi$'s), CUSB can measure the BR($\phi \to f_0\gamma$) (using the charged pion decay mode), from 37% to 1.6% accuracy over the signal BR range of 1×10^{-5} to 2.5×10^{-4} if the BR of direct $\phi \to \pi^+\pi^-\gamma$ is the one expected theoretically. If the direct $\phi \to \pi^+\pi^-\gamma$ BR is at the experimental limit CUSB can measure to 37% accuracy only if the signal BR is 1×10^{-5}. In this decay again CUSB suffers from lack of hermeticity, as well as lack of momentum information, so that the dominant background come from the $\pi\rho$ final states which give $\pi^+\pi^-\pi^0$ where one of the photons escape the detector, and one cannot apply energy-momentum constraint arising from a real ρ having been produced.

Table IIa. BR and ϵ for charged signal and backgrounds in CUSB, KLOE and CMD2

PROCESS	BR	$\epsilon_{(CUSB)}$	$\epsilon_{(KLOE)}$	$\epsilon_{(CMD2)}$
$\phi \to f_0\gamma \to \pi^+\pi^-\gamma$	$(0.52 \to 130)\times 10^{-6}$	7.4×10^{-2}	7.4×10^{-1}	6.4×10^{-1}
$\phi \to \pi^+\pi^-\gamma$	$(2.4 \to 700)\times 10^{-5}$	1.5×10^{-4}	1.2×10^{-3}	1.2×10^{-3}
$\phi \to \pi^0\rho^0 \to \pi^+\pi^-\gamma$	4.3×10^{-2}	7.2×10^{-3}	$<3\times 10^{-6}$	$<3\times 10^{-6}$
$\phi \to \pi^\pm\rho^\mp \to \pi^+\pi^-\gamma$	8.6×10^{-2}	1.7×10^{-3}	$<3\times 10^{-6}$	$<3\times 10^{-6}$
$\phi \to \pi^+\pi^-\pi^0 \to \pi^+\pi^-\gamma$	1.9×10^{-2}	1.3×10^{-3}	$<3\times 10^{-6}$	$<3\times 10^{-6}$

The KLOE simulation is still in progress,[12] however because of KLOE's hermeticity, and the fact that one measures the charged particles' momenta, applying kinematical constraints make background processes (2) and (3) negligible relative to (1) despite their larger BR's. The KLOE column in tables IIa and IIb are obtained by simply considering geometry and assuming 0.45% momentum resolution. The fractional accuracy achievable has been increased by a factor two, to roughly account for various uncertainties not yet fully evaluated. Similar results are obtained for the CMD2 Detector[5] which is also supposed to be hermetic. While its momentum resolution and energy resolution are a factor of two worse than KLOE's, for this signal it is not important because of the width of the f_0. With the charged channel, using general purpose detectors, one expects a very good BR determination over the whole range of signal and background BR examined. However, in this channel, extra background can arise from radiative corrections, coupling of the initial e^+e^- state to the tail of the ρ, which can only be removed by comparing the BR's values to the measurements obtained from using the neutral decay mode.

Table IIb. Fractional error in BR($\phi \to f_0\gamma$) for CUSB, KLOE and CMD2

BR($\phi \to f_0\gamma$)	BR($\phi \to \pi^+\pi^-\gamma$)	δ(BR)/BR CUSB	δ(BR)/BR KLOE	δ(BR)/BR CMD2
1.0×10^{-6}	2.4×10^{-5}	3.95	0.033	0.037
1.0×10^{-5}	2.4×10^{-5}	0.37	0.008	0.008
2.5×10^{-4}	2.4×10^{-5}	0.016	0.001	0.002
1.0×10^{-6}	7.0×10^{-3}	3.95	0.081	0.096
1.0×10^{-5}	7.0×10^{-3}	0.37	0.011	0.013
2.5×10^{-4}	7.0×10^{-3}	0.016	0.001	0.002

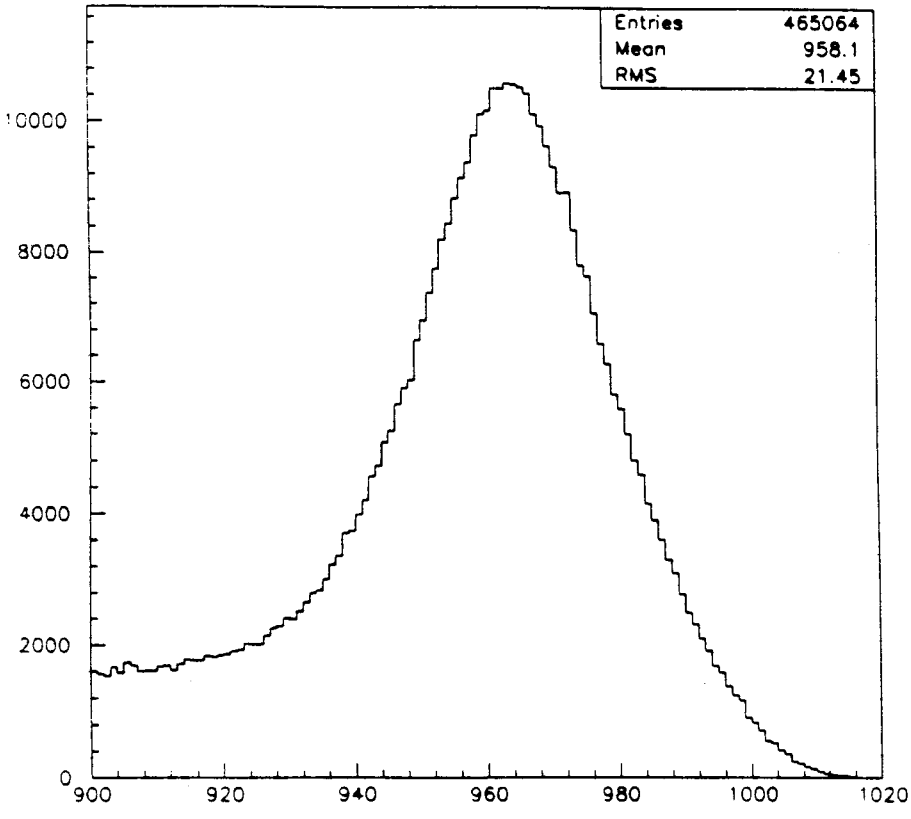

Figure 2. $M_{\pi^+\pi^-}$-spectrum in KLOE.

Figure 2 shows the $M_{\pi^+\pi^-}$-spectrum in KLOE from one year's run with BR($\phi \to f_0\gamma$)= 2.5×10^{-4} and BR($\phi \to \pi^+\pi^-\gamma$)= 7×10^{-3}. The figure shows the advantage of having a momentum resolution negligible compared to the signal width, see the corresponding figure for CMD2 in ref. 5.

4. $\phi \to \eta'\gamma$

We have also considered the accuracy achievable by KLOE in the measurement of BR($\phi \to \eta'\gamma$), for an equal running period. This ϕ decay mode has never been seen; the experimental upper limit is 4.1×10^{-4}. Measurement of the BR of this mode will shed light on the gluonium content, $Z_{\eta'}$, of the η'.[15] The rate of this decay is proportional to the amplitude, $Y_{\eta'}$, of the $\bar{s}s$ component of its wave function,

$$\frac{\Gamma(\phi \to \eta'\gamma)}{\Gamma(\phi \to \eta\gamma)} = \left(\frac{Y_{\eta'}}{Y_\eta}\right)^2 \left(\frac{k_{\eta'}}{k_\eta}\right)^3 \sim 4.6 \times 10^{-3} \left(\frac{Y_{\eta'}}{Y_\eta}\right)^2. \qquad (4.1)$$

To give an idea of the expected order of magnitude of the branching ratio, for $Z_{\eta'} = 0$ and the $\eta - \eta'$ mixing angle $\theta_p = -20°$,[16] BR($\phi \to \eta'\gamma$) $\sim 1.2 \times 10^{-4}$.

The signature for $\phi \to \eta'\gamma$, $\eta' \to \eta\pi^+\pi^-$ and $\eta \to \gamma\gamma$ is: a pair of charged pions, two photons whose invariant mass equals that of the η, and one low energy photon. The invariant mass of all particles must equal the ϕ mass. By applying these criteria, the efficiency×acceptance for the signal in KLOE is 74.5%. The possible background events are from:

1. $\phi \to \eta\gamma$, BR=$(1.28 \pm 0.06) \times 10^{-2}$, $\eta \to \pi^+\pi^-\pi^0$, product BR 3.0×10^{-3}. Overall kinematical constraint pushes the background down so that the efficiency×acceptance for this background in KLOE is 2.58×10^{-3}.
2. $\phi \to \omega\gamma$, BR 5%, $\omega \to 3\pi$, product BR=4.4×10^{-2}. Overall kinematical constraint results in an efficiency×acceptance for this background in KLOE of 5.94×10^{-3}.
3. $\phi \to \pi^0\rho^0 \to \pi^0\pi^+\pi^-\gamma$, product BR=$(4.8 \pm 0.6) \times 10^{-3}$. Overall kinematical constraint results in an efficiency×acceptance for this background in KLOE of 5.58×10^{-3}.

Again we calculated the fractional accuracy achievable in KLOE for the measurement of this BR. The results are tabulated in table III. We note that in the first year's run, KLOE can measure, at a sixteen sigma significance, a BR one/tenth of the BR expected from eq. 4.1.

Table III. Fractional error in BR($\phi \to \eta'\gamma$) for KLOE

BR($\phi \to \eta'\gamma$)	δ(BR)/BR
1.0×10^{-5}	0.0634
4.1×10^{-4}	0.0025

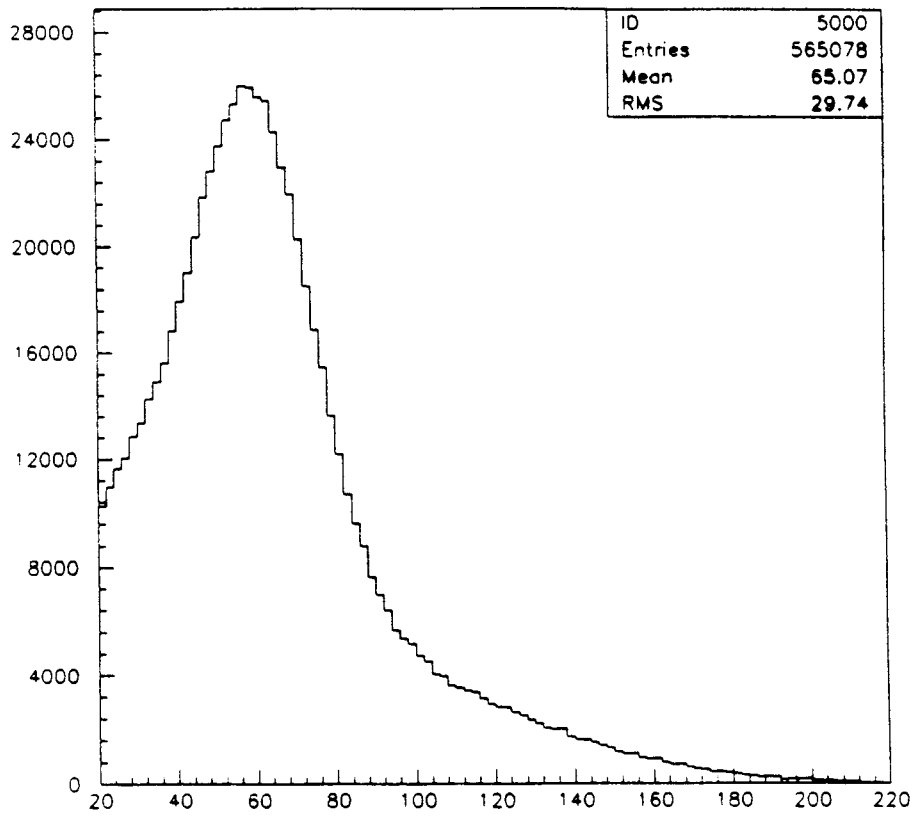

Figure 3. Photon Spectrum in KLOE from $\phi \rightarrow \eta' \gamma$.

5. CONCLUSION

We have studied the experimental problems associated with measuring ϕ radiative decays by choosing two typical and interesting ones: $\phi \rightarrow f_0 \gamma$, where the f_0 decays to two neutral pions or two charged pions, and $\phi \rightarrow \eta' \gamma$. We simulated the signal and the expected background in a neutral particle spectrometer: CUSB-II, found the reaction easily measurable in one year's running time ($\sim 5 \times 10^9 \phi$'s). We also made estimates for the case of two general purpose detectors: KLOE and CMD2, and found the hermeticity of these detectors render the measurements almost trivial. However, the charged modes are subject to continuum background which we discuss in detail in a separate paper.[17] We found the η' search using KLOE relatively easy. Implementation of both types of detectors at DAΦNE is highly desirable and promises to produce good physics.

6. APPENDIX

For completeness, in this Appendix we give the full angular distributions of the ϕ decay to $\pi\pi\gamma$ through a virtual ρ, in other words, the matrix element resulting from calculating the Feynman diagrams starting with e^+e^- rather than with a resonance in an averaged polarization state. This yields the same integrated rates as found previously (Bramon, Grau, and Pancheri[9]) but, in addition, the correct angular distributions, which are necessary for Monte Carlo simulations of these processes.

In general, the full angular dependence of a ϕ decay process, where the ϕ originates in an e^+e^- collision, can be derived by replacing the ϕ polarization vector ϵ^*_μ, in an amplitude given for ϕ decay, by $\bar{e}\gamma_\mu e$, or, if

$$A(\phi \to XYZ) = \epsilon^{*\mu} R_\mu \tag{6.1}$$

we have

$$|\mathcal{A}(e^+e^- \to \phi \to XYZ)|^2_{e^+e^- \text{ spin avg.}} = \left(p^\mu p'^\nu + p'^\mu p^\nu - g^{\mu\nu} p\cdot p'\right) R_\mu R_\nu \tag{6.2}$$

where p and p' are the electron and positron 4-momenta. Thus, the decay width of a ϕ originating in e^+e^- collisions is:

$$\mathrm{d}\Gamma(\phi_{e^+e^-} \to XYZ) = \mathrm{d}\sigma(e^+e^- \to \phi \to XYZ)\,\frac{\Gamma(\phi \to \text{everything})}{\sigma_{\text{prod}}(e^+e^- \to \phi)} = \frac{\mathcal{K}|\mathcal{A}|^2}{M_\phi^2}, \tag{6.3}$$

where $\mathcal{K}$ is the usual kinematic factor for decays,

$$\mathcal{K} = \frac{1}{64\pi^3}\frac{1}{M_\phi^2}\mathrm{d}E_1\mathrm{d}E_2\frac{\mathrm{d}\phi_1}{2\pi}\frac{\mathrm{d}\cos\theta_1}{2}\frac{\mathrm{d}\phi_2}{2\pi} \tag{6.4}$$

with an extra factor of 1/2 if there are two identical particles in the final state. The point of this notation is to isolate the changes needed to go from previous calculations to ones taking into account the ϕ polarization acquired from the e^+e^- collision. These are simply: changing from eq. (6.1) to (6.2); the factor of $\frac{1}{M_\phi^2}$ in eq. (6.3), and the missing polarization averaging factor of $\frac{1}{3}$ in eq. (6.4).

We then have, for $\phi \to \rho\pi \to \pi^+\pi^-\gamma$

$$R_\mu = \left(\frac{\epsilon G^2 e}{3g\sqrt{2}}\right)\frac{\epsilon_{\mu\alpha\beta\gamma}(q_\alpha + p^+_\alpha)q^*_\beta\epsilon_{\gamma\delta\epsilon\rho}q_\delta(q_\epsilon + p^+_\epsilon)\epsilon_\rho}{M_\rho^2 - (q+p^+)^2 - iM_\rho\Gamma_\rho} + (p^+ \leftrightarrow p^-) \tag{6.5}$$

where $G = \frac{3\sqrt{2}g^2}{4\pi^2 f_\pi}$, f_π is the pion decay constant, 132 MeV, g=4.2, and $\epsilon = -0.059$ (see Ref. 9 for further details).

The most compact way to display our result, then, is to borrow the notation of Creutz and Einhorn,[18] correcting a factor of 1/2 and some signs that we find ourselves in disagreement with:

$$|\mathcal{A}|^2 = \left(\frac{\epsilon G^2 e}{3g\sqrt{2}}\right)^2 s^2 \times \left[\frac{1}{2}|H_1|^2\beta_\pi^2 t\sin^2\theta_\gamma\sin^2\theta_{\pi\gamma}\right.$$

$$+\frac{1}{2}|H_2|^2\beta_\pi^4 t\sin^2\theta_{\pi\gamma}\left[\cos^2\theta_{\pi\gamma}+\frac{t}{s}\sin^2\theta_{\pi\gamma}-(\cos\theta_\gamma\cos\theta_{\pi\gamma}-\sqrt{\frac{t}{s}}\sin\theta_\gamma\sin\theta_{\pi\gamma}\cos\phi)^2\right]$$

$$+|H_3|^2(1+\cos^2\theta_\gamma)/(2s)$$

$$+\mathrm{Re}(H_1H_2^*)\beta_\pi^3 t\sin\theta_\gamma\sin^2\theta_{\pi\gamma}\left[\sqrt{\frac{t}{s}}\sin\theta_{\pi\gamma}\cos\theta_\gamma\cos\phi+\sin\theta_\gamma\cos\theta_{\pi\gamma}\right]$$

$$+\mathrm{Re}(H_1H_3^*)\beta_\pi\sqrt{\frac{t}{s}}\sin\theta_\gamma\cos\theta_\gamma\sin\theta_{\pi\gamma}\cos\phi$$

$$\left.+\mathrm{Re}(H_2H_3^*)\beta_\pi^2\sqrt{\frac{t}{s}}\sin\theta_{\pi\gamma}\left[\sin\theta_\gamma\cos\theta_\gamma\cos\theta_{\pi\gamma}\cos\phi+\sqrt{\frac{t}{s}}\sin\theta_{\pi\gamma}(1-\sin^2\theta_\gamma\cos^2\phi)\right]\right] \tag{6.6}$$

where t is the four-momentum squared of the dipion system, s of the dilepton system, and β_π the velocity of the pions in the dipion rest frame, $\beta_\pi = \sqrt{1-\xi/(1-x)}$. ϕ is the angle between the $e^+e^-\gamma$ plane and the $\pi^+\pi^-$ plane in the lab frame or the dipion rest frame; θ_γ is the photon-beam angle in the lab frame, and $\theta_{\pi\gamma}$ is the angle between the pions and the photon *in the dipion rest frame* related to the pion energy E_π in the lab frame by

$$y = 1-\frac{x}{2}\left(1-\cos\theta_{\pi\gamma}\sqrt{1-\frac{\xi}{1-x}}\right). \tag{6.7}$$

where $x = 2E_\gamma/\sqrt{s}$, $y = 2E_\pi/\sqrt{s}$, and $\xi = 4m_\pi^2/s$. E_γ and E_π are the energies of the photon and one of the pions in the lab frame. The H_i are general form factors which in our case are given by

$$H_i = \frac{h_i}{M_\rho^2+2M_\phi E_\pi - M_\phi^2 - m_\pi^2 - iM_\rho\Gamma_\rho} + (\pi^+ \leftrightarrow \pi^-) \tag{6.8}$$

with

$$h_1 = -\frac{sx}{8}, h_2 = \frac{sx}{8}, h_3 = \frac{s^2}{8}(2x^2+x\xi-2x-2y^2+2y). \tag{6.9}$$

The h_i and $h_i(\pi^+ \leftrightarrow \pi^-)$ come from the direct and crossed diagrams, and the

separate contributions from these diagrams and their interference may be easily written in terms of the h_i. Combining all these equations then gives the full angular dependence for $\phi_{e^+e^-} \to \pi^+\pi^-\gamma$ via a virtual ρ; $\phi_{e^+e^-} \to \pi^0\pi^0\gamma$ is identical except for the factor of 1/2 in $\mathcal{K}$. The angle ϕ can be trivially integrated over by replacing $\cos^2\phi$ by $\frac{1}{2}$, and $\cos\phi$ by zero (after first carrying out the appropriate squares).

In figures 4 and 5 we show two views of the angular distribution: $\mathrm{d}^2\sigma/\mathrm{dE}_\gamma \mathrm{d}\cos\theta_{\gamma,\mathrm{beam}}$ vs E_γ, $\cos\theta_{\gamma,\mathrm{beam}}$, and $\mathrm{d}^2\sigma/\mathrm{dE}_\gamma \mathrm{d}\cos\theta_{\pi\gamma}$ vs E_γ, $\cos\theta_{\pi\gamma}$ for $\phi_{e^+e^-} \to \rho\pi \to \pi^0\pi^0\gamma$. The angle $\theta_{\pi\gamma}$ used here is the angle between the pions and the photon *in the dipion rest frame.*

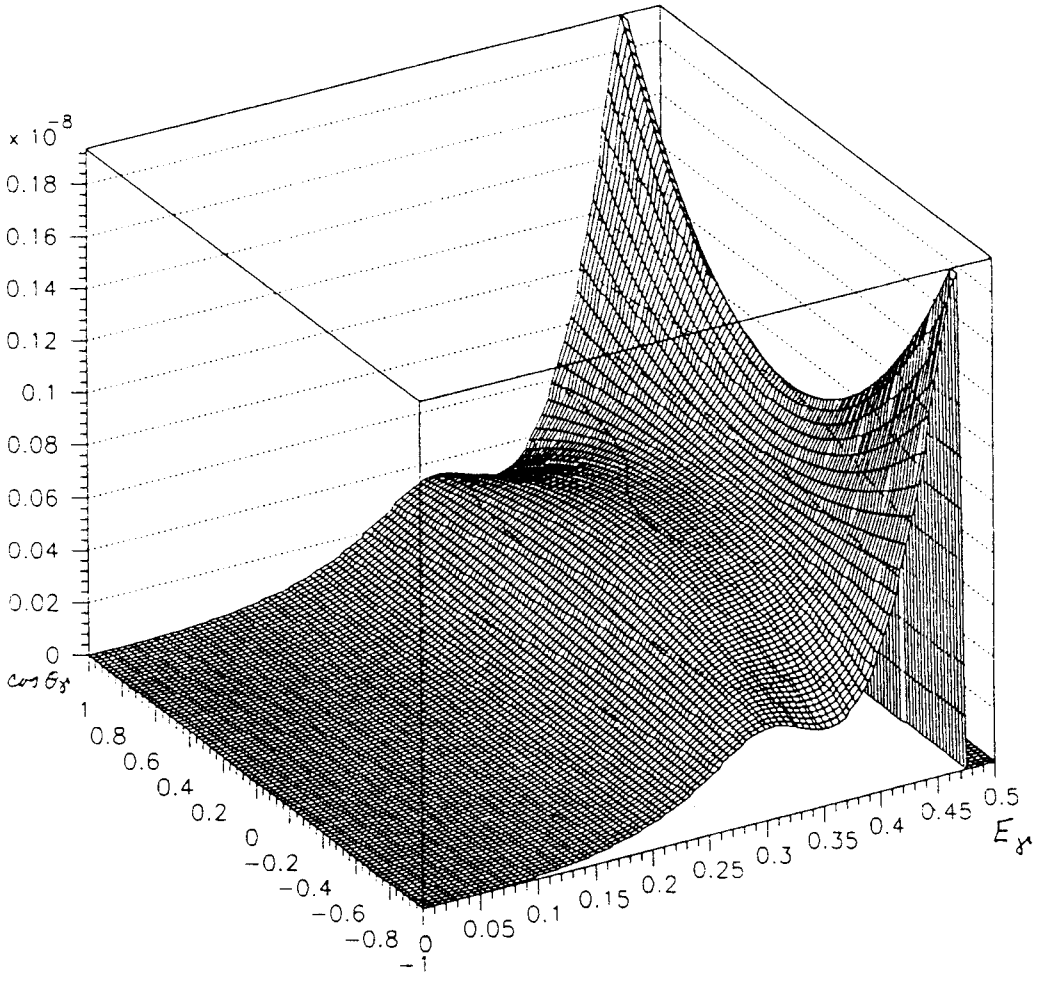

Fig. 4. $\mathrm{d}^2\sigma/\mathrm{dE}_\gamma \mathrm{d}\cos\theta_{\gamma,\mathrm{beam}}$ vs E_γ, $\cos\theta_{\gamma,\mathrm{beam}}$

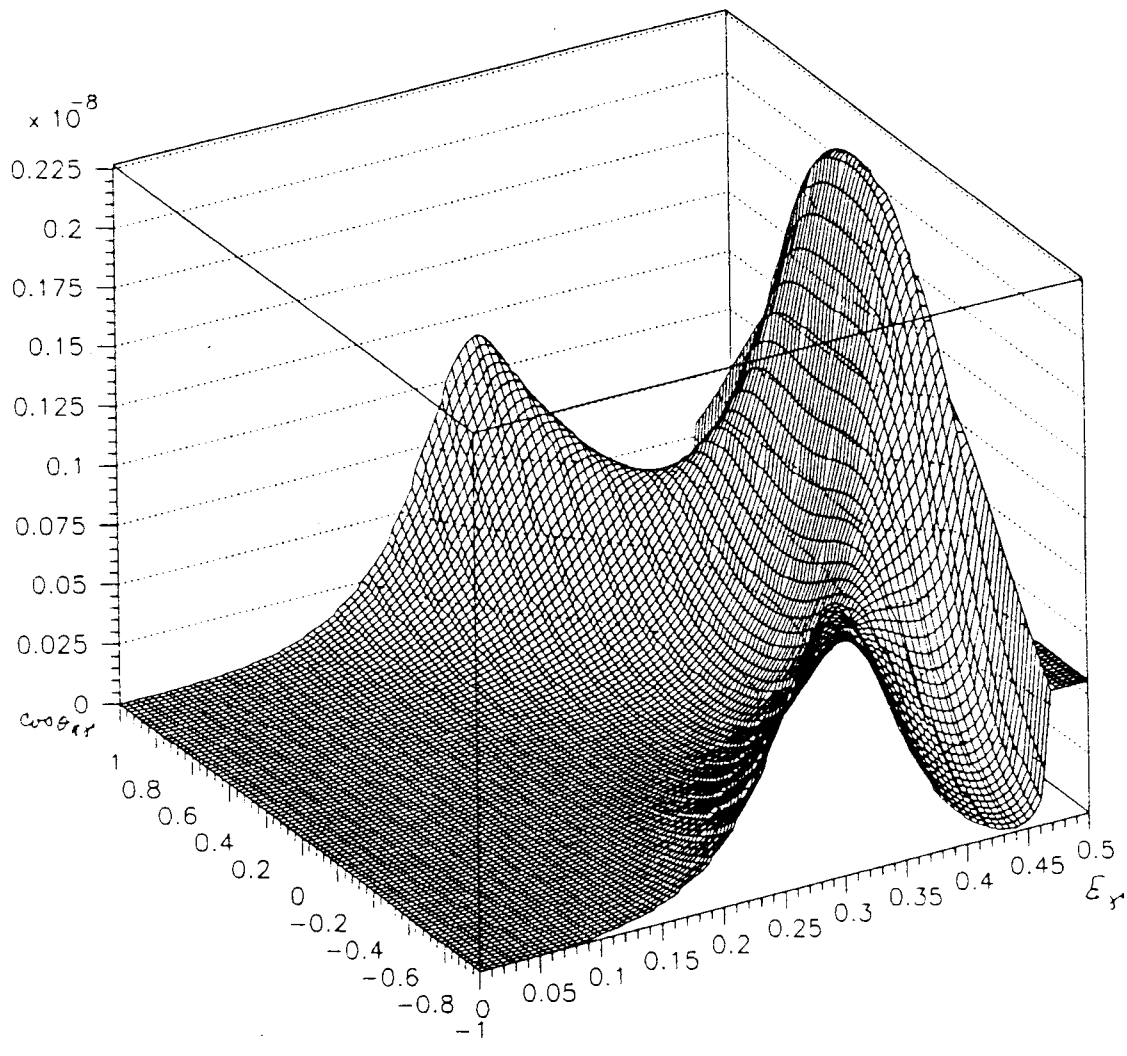

Fig. 5. $d^2\sigma/dE_\gamma d\cos\theta_{\pi\gamma}$ vs E_γ, $\cos\theta_{\pi\gamma}$

ACKNOWLEDGEMENTS

We wish to thank Paolo Franzini for discussions and help in preparing this paper.